

$^{12}\text{C}(^{18}\text{O},\alpha p\gamma)$ **2020Wi11**

Type	Author	History	Citation	Literature Cutoff Date
Full Evaluation	M. Shamsuzzoha Basunia, Anagha Chakraborty		NDS 205,1 (2025)	31-May-2025

Adapted/Edited the XUNDL dataset compiled by J. Chen (NSCL, MSU), December 8, 2020.

2020Wi11: ^{18}O beam, E=48 MeV, was produced from the TRIUMF-ISAC facility. Targets were a thin and a backed foil of natural carbon. γ rays were detected with the TIGRESS array consisting of 13 Compton-suppressed HPGe clovers and charged particles were detected with a 38-element array of CsI(Tl) scintillators. Measured $E\gamma$, $I\gamma$, $\gamma\gamma$ -coin, particle- γ -coin, $\gamma(\theta)$. Deduced excited level energies, spin, parity, lifetimes, γ -ray multipolarities, transition strengths. Shell-model calculations.

Other reactions: $^{12}\text{C}, ^{16}\text{O}(^{16}\text{O},\text{X})$ at E=70-130 MeV ([1986Ik03](#)).

 ^{25}Na Levels

E(level) [†]	J^π [#]	$T_{1/2}$ ^{&}	Comments
0 ^c	5/2 ⁺ [@]		
(92 ^f) 3	3/2 ⁺ [@]		E(level): from energy difference of transitions depopulating 2791 level. Not observed in this work (2020Wi11).
1072 ^f 3	1/2 ⁺ [@]	>0.55 ps	$T_{1/2}$: from $\tau>900$ fs.
2204 ^f 3	3/2 ⁺ [@]	18 fs 8	$T_{1/2}$: from $\tau=26$ fs 11 .
2419.7 ^c 8	(9/2 ⁺)	159 ^a fs 28	$T_{1/2}$: from $\tau=230$ fs 40 .
2791.1 ^d 9	7/2 ⁺	104 ^a fs 14	J^π : from literature in 2020Wi11 . $T_{1/2}$: from $\tau=150$ fs 20 .
3356.1 ^e 22	(7/2 ⁺) [@]	<34 fs	$T_{1/2}$: from $\tau<49$ fs.
3460.8 ^c 9	(9/2 ⁺)	132 ^a fs 21	$T_{1/2}$: from $\tau=190$ fs 30 .
3964 4	(1/2,3/2,5/2 ⁺)	<173 fs	$T_{1/2}$: from $\tau<250$ fs.
4000.0 ^d 9	(9/2 ⁺)	62.4 fs 49	J^π : from literature in 2020Wi11 . $T_{1/2}$: from $\tau=90$ fs 7 .
4006 4	(1/2,3/2)	62 fs 35	$T_{1/2}$: from $\tau=90$ fs 50 .
4295 4	1/2 ⁺ [@]	<20 fs	$T_{1/2}$: from $\tau<29$ fs.
4967.2 ^c 9	(11/2 ⁺) [@]	49.9 ^a fs 42	$T_{1/2}$: from $\tau=72$ fs 6 .
5231.4 ^e 22	(7/2,9/2)	<10 fs	$T_{1/2}$: from $\tau<15$ fs.
5388.1 ^b 14	(11/2 ⁺)	<2.8 fs	$T_{1/2}$: from $\tau<4$ fs.
5749 4	(9/2,11/2,13/2)	<194 fs	$T_{1/2}$: from $\tau<280$ fs.
5848 3		<52 fs	$T_{1/2}$: from $\tau<75$ fs.
6271 ^f 3	(9/2,11/2)	<26 fs	$T_{1/2}$: from $\tau<37$ fs.
6381 3	(9/2,11/2,13/2)	<6.2 fs	$T_{1/2}$: from $\tau<9$ fs.
6582 3		<28 fs	J^π : (11/2 ⁻) from literature (Ph.D. thesis) for a 6.55 MeV level. $T_{1/2}$: From $\tau<40$ fs.
6737.0 14	(13/2 ⁺)	<2.8 fs	$T_{1/2}$: from $\tau<4$ fs.
6856.1 ^b 16	(13/2 ⁺)	42 fs 28	$T_{1/2}$: from $\tau=60$ fs 40 .
7218 ^f ^d 4	(9/2,11/2,13/2)	<97 fs	$T_{1/2}$: from $\tau<140$ fs.
7625 ^f ^c 4	(11/2,13/2)	<52 fs	$T_{1/2}$: from $\tau<75$ fs.

[†] From a least-squares fit to γ -ray energies. The bands proposed in [2020Wi11](#) are labelled as “sequence” in this dataset. Same spin is proposed for two states by the authors doe most of their proposed bands.

[‡] Newly identified level in [2020Wi11](#) compared to the known excited levels of ^{25}Na prior to their work.

[#] As given in [2020Wi11](#) based on $\gamma(\theta)$ and γ de-excitation pattern, unless otherwise noted.

[@] From Adopted Levels. In [2020Wi11](#), it was quoted from the literature.

[&] From DSAM in [2020Wi11](#). Limit reported to a 90% confidence level. Authors note that most of their mean lifetime values are lower than those reported in $^9\text{Be}(^{18}\text{O},\text{pny})$ ([2015Vo12](#)), this is most likely a systematic effect resulting from the use of two stopping models in this work compared to $^9\text{Be}(^{18}\text{O},\text{pny})$ that used the SRIM model exclusively.

$^{12}\text{C}(^{18}\text{O},\alpha\gamma)$ 2020Wi11 (continued) **^{25}Na Levels (continued)**^a Corrected for feeding from an observed transition (2020Wi11).^b Seq.(A): based on 5388, (11/2⁺).^c Seq.(B): based on g.s., 5/2⁺.^d Seq.(C): based on 2791, 7/2⁺.^e Seq.(D): based on 3356, (7/2⁺).^f Seq.(E): based on 92, 3/2⁺. **$\gamma(^{25}\text{Na})$**

E_γ	$I_\gamma^{\frac{1}{2}}$	$E_i(\text{level})$	J_i^π	E_f	J_f^π	Mult. [#]	Comments
669.1 7	2.2 3	3460.8	(9/2 ⁺)	2791.1	7/2 ⁺		$A_2=-0.4$ 2
967.3 9	1.1 3	4967.2	(11/2 ⁺)	4000.0	(9/2 ⁺)		$A_2=-0.2$ 5
980.4 5	17.0 14	1072	1/2 ⁺	92?	3/2 ⁺		$A_2=-0.7$ 3
1041.3 4	42.7 11	3460.8	(9/2 ⁺)	2419.7	(9/2 ⁺)	D+Q @	$A_2=+0.20$ 6; $A_4=+0.12$ 7
1131.8 4	6.9 12	2204	3/2 ⁺	1072	1/2 ⁺		$A_2=-0.1$ 3
1209.0 4	13.5 10	4000.0	(9/2 ⁺)	2791.1	7/2 ⁺		$A_2=-0.31$ 9
1348.9 [†] 13	2.1 5	6737.0	(13/2 ⁺)	5388.1	(11/2 ⁺)		$A_2=+0.3$ 3
1467.9 10	2.6 4	6856.1	(13/2 ⁺)	5388.1	(11/2 ⁺)		$A_2=-0.6$ 3
1506.2 6	24.4 10	4967.2	(11/2 ⁺)	3460.8	(9/2 ⁺)	D+Q @	$A_2=-0.54$ 13; $A_4=+0.24$ 16
1579.1 13	2.8 4	4000.0	(9/2 ⁺)	2419.7	(9/2 ⁺)		$A_2=+0.0$ 3
1770.7 16	6.4 8	6737.0	(13/2 ⁺)	4967.2	(11/2 ⁺)		$A_2=-0.3$ 2
1875.0 12	4 2	5231.4	(7/2,9/2)	3356.1	(7/2 ⁺)		$A_2=+0.3$ 2
2419.6 11	100 3	2419.7	(9/2 ⁺)	0	5/2 ⁺	Q @	$A_2=+0.13$ 6; $A_4=-0.27$ 7
2441 [†] 3	0.9 3	5231.4	(7/2,9/2)	2791.1	7/2 ⁺		$A_2=-0.9$ 9
2548.0 12	14.0 9	4967.2	(11/2 ⁺)	2419.7	(9/2 ⁺)		$A_2=-0.03$ 13
2658 [†] 4	2.7 5	7625	(11/2,13/2)	4967.2	(11/2 ⁺)		$A_2=-0.6$ 4
2699 3	1.8 4	2791.1	7/2 ⁺	92?	3/2 ⁺		$A_2=+0.9$ 3
2790.8 13	19.2 15	2791.1	7/2 ⁺	0	5/2 ⁺		$A_2=+0.39$ 14
2891 3	2.6 9	3964	(1/2,3/2,5/2 ⁺)	1072	1/2 ⁺		$A_2=+0.0$ 5
2924 [†] 5	1.8 5	6381	(9/2,11/2,13/2)	3460.8	(9/2 ⁺)		$A_2=-0.6$ 8
2933 3	2.6 9	4006	(1/2,3/2)	1072	1/2 ⁺		$A_2=-0.8$ 6
2968.4 15	17.0 10	5388.1	(11/2 ⁺)	2419.7	(9/2 ⁺)		$A_2=-0.15$ 13
3058 3	1.4 3	5848		2791.1	7/2 ⁺		$A_2=+0.9$ 5
3120 4	2.0 4	6582		3460.8	(9/2 ⁺)		$A_2=-0.2$ 7
3218 [†] 4	1.2 3	7218	(9/2,11/2,13/2)	4000.0	(9/2 ⁺)		$A_2=+0.6$ 4
3222 3	3.0 10	4295	1/2 ⁺	1072	1/2 ⁺		$A_2=-0.4$ 7
3275 [†] 6	1.2 4	6737.0	(13/2 ⁺)	3460.8	(9/2 ⁺)		$A_2=-0.1$ 10
3329 [†] 4	1.6 3	5749	(9/2,11/2,13/2)	2419.7	(9/2 ⁺)		$A_2=+0.1$ 4
3355 3	4.5 16	3356.1	(7/2 ⁺)	0	5/2 ⁺		$A_2=-0.2$ 3
3395 [†] 5	1.5 4	6856.1	(13/2 ⁺)	3460.8	(9/2 ⁺)		$A_2=-0.7$ 7
3427 4	1.7 3	5848		2419.7	(9/2 ⁺)		$A_2=+0.1$ 4
3462 [†] 3	3.2 11	3460.8	(9/2 ⁺)	0	5/2 ⁺		$A_2=-0.1$ 7
3480 [†] 4	1.0 2	6271	(9/2,11/2)	2791.1	7/2 ⁺		$A_2=-0.3$ 7
3851 ^{†&} 5	<0.4	6271	(9/2,11/2)	2419.7	(9/2 ⁺)		
3958 4	3.7 4	6381	(9/2,11/2,13/2)	2419.7	(9/2 ⁺)		$A_2=-0.1$ 2
4163 4	2.7 3	6582		2419.7	(9/2 ⁺)		$A_2=-0.1$ 3
4313 [†] 3	5.3 4	6737.0	(13/2 ⁺)	2419.7	(9/2 ⁺)	Q	$A_2=+0.3$ 2
4436 3	3.1 3	6856.1	(13/2 ⁺)	2419.7	(9/2 ⁺)	Q	$A_2=+0.5$ 4
4796 [†] 9	0.6 2	7218	(9/2,11/2,13/2)	2419.7	(9/2 ⁺)		$A_2=-1.4$ 13

Continued on next page (footnotes at end of table)

 $^{12}\text{C}(^{18}\text{O},\alpha\gamma)$ 2020Wi11 (continued)

 $\gamma(^{25}\text{Na})$ (continued)

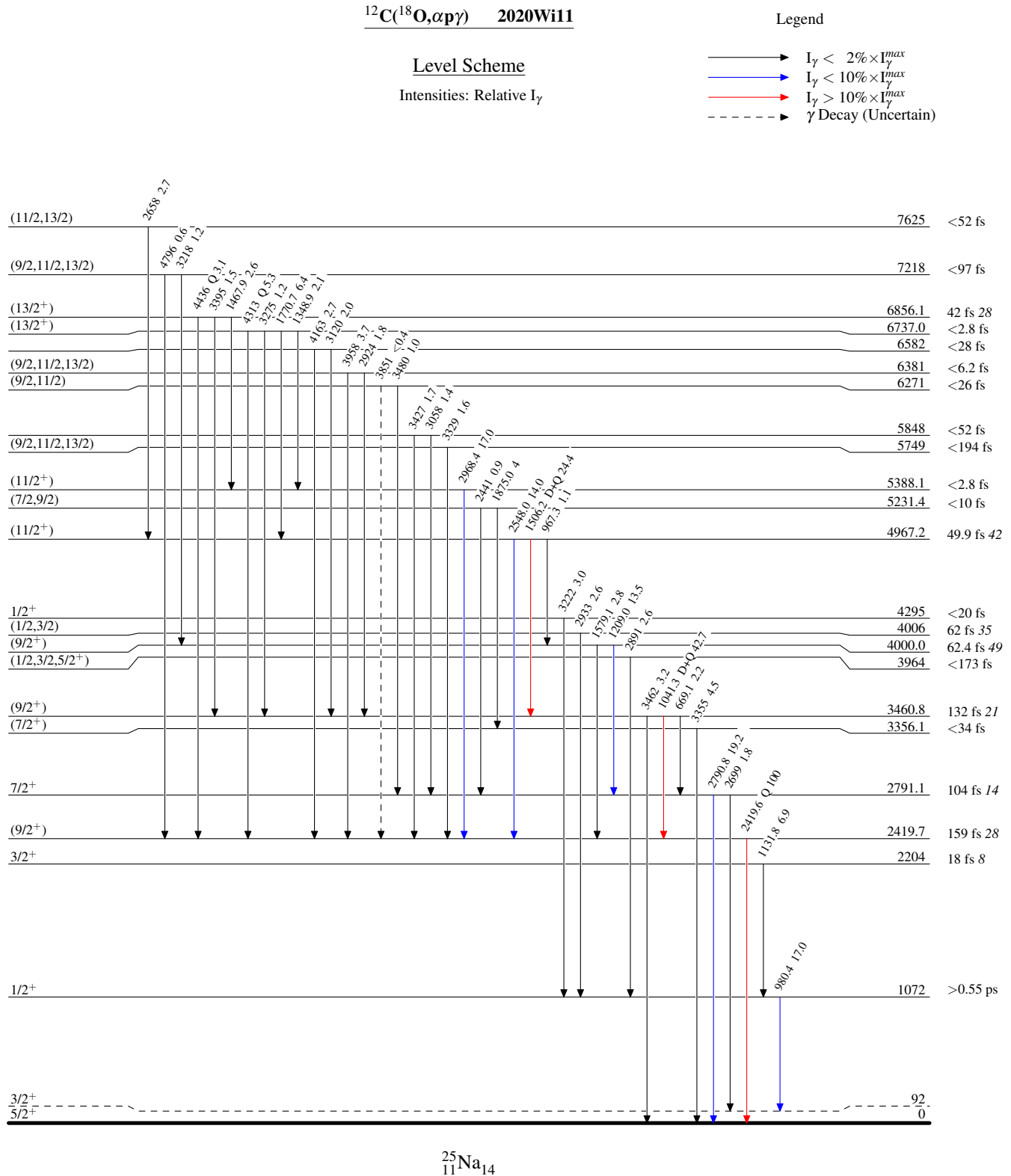
[†] New transition (2020Wi11).

[‡] Relative intensity with respect to $I\gamma(2419.6\gamma)=100$. In 2020Wi11, relative intensities were reported with respect to $I\gamma(2419.6\gamma)=1.00$.

[#] From $\gamma(\theta)$ (2020Wi11), proposed by the evaluator, except where otherwise noted.

[@] Assignment in 2020Wi11, based on their $\gamma(\theta)$ data.

[&] Placement of transition in the level scheme is uncertain.



$^{12}\text{C}({}^{18}\text{O},\alpha p\gamma) \quad 2020\text{Wi11}$ Seq.(B): Based on g.s., $5/2^+$ Seq.(A): Based on 5388,
($11/2^+$)(11/2,13/2) 7625Seq.(C): Based on 2791, $7/2^+$ (9/2,11/2,13/2) 7218Seq.(D): Based on 3356,
($7/2^+$)(7/2,9/2) 5231.4Seq.(E): Based on 92,
 $3/2^+$ 3/2⁺ 2204